Biophysical Characterization of Cyclic Nucleotide Phosphodiesterases

Andreas Hofmann,*,1 Sergey Tarasov,† Melissa Grella,*,2 Sergei Ruvinov,‡
Fahd Nasr,§ Witold Filipowicz,§ and Alexander Wlodawer*

*Protein Structure Section, Macromolecular Crystallography Laboratory, and †Structural Biophysics Laboratory,
National Cancer Institute at Frederick, Frederick, Maryland 21702; ‡Laboratory of Biochemistry,
Center for Cancer Research, National Cancer Institute, Bethesda, Maryland 20892; and
§Friedrich Miescher Institute for Biomedical Research, 4002 Basel, Switzerland

We have compared selected biophysical properties of three phosphodiesterases, from *Arabidopsis thaliana, Saccharomyces cerevisiae,* and *Escherichia coli.* All of them belong to a recently identified family of cyclic nucleotide phosphodiesterases. Experiments elucidating folding stability, protein fluorescence, oligomerization behavior, and the effects of substrates were conducted, revealing differences between the plant and the yeast protein. According to CD spectroscopy, the latter protein exhibits an $(\alpha + \beta)$ fold rather than an (α/β) fold as found with CPDase (*A. thaliana*). The redox-dependent structural reorganization recently found for the plant protein by X-ray crystallography could not be detected by CD spectroscopy due to its only marginal effect on the total percentage of helical content. However, in the present study a redox-dependent effect was also observed for the yeast CPDase. The enzymatic activity of wild type CPDase (*A. thaliana*) as well as of four mutants were characterized by isothermal titration calorimetry and the results prove the requirement of all four residues of the previously identified tandem signature motif for the catalytic function. Within the comparison of the three proteins in this study, the PDase Homolog/RNA ligase (*E. coli*) shares more similarities with the plant than with the yeast protein.

Key Words: cyclic nucleotide phosphodiesterases; isothermal titration calorimetry; sedimentation equilibrium analysis; ultracentrifugation; urea denaturation.

Cyclic nucleotide phosphodiesterases (CPDases) characterized in wheat [L8], *Arabidopsis thaliana* (1, 2), and yeast (1, 3, 4), constitute one group within a large family of proteins that includes at least four different classes of enzymes having cyclic nucleotide phosphodiesterase or related activities. On the primary structure level, enzymes of this family consist of chains containing approximately 200 amino acids and share a tandem signature motif, H-Φ-T/S-Φ, with Φ being a hydrophobic residue (L, V, I) (4).

A variety of different cyclic nucleotides serve as substrates for these enzymes, among them ADP-ribose 1″,2″-cyclic phosphate (Appr > p), which is a product generated during tRNA splicing in yeast, plants and also vertebrates (1, 5, 6). Further processing, catalyzed by a CPDase, requires cleavage of the 2″-phosphoester linkage and yields ADP-ribose 1″-phosphate (Appr-1″p) (2, 7). The CPDase was purified originally from wheat germ as an enzyme catalyzing hydrolysis of nucleoside 2′,3′-cyclic phosphates (N > p) to nucleoside 2′-phosphates (N-2′p) (8). Further characterization of CPDases from wheat and *A. thaliana* revealed that the enzyme also hydrolyses Appr > p to Appr-2′p (1, 2). A partially purified enzyme from yeast was found to use specifically Appr > p, but not N > p, as a substrate (1). However, the CPDase gene in *Saccharomyces cerevisiae* has been identified recently and it was shown that the recombinant yeast protein hydrolyses both Appr > p and N > p (3, 4). It seems likely that the specificity of this enzyme is controlled by some additional proteins or other factors. The PDase Homolog/RNA ligase (*E. coli*) belongs to a second class of this protein family comprised of bacterial and archaeal RNA ligases (9) which are able to ligate tRNA half molecules containing 2′,3′-cyclic phosphate and 5′-hydroxyl termini to products containing a 2′,5′-phosphodiester linkage (9, 10). Physiological substrates of these enzymes are not known. Remarkably, cyclic phosphodiesterase activity

of these enzymes has not been reported so far; however, the reaction they catalyze must involve hydrolysis of a 2′,3′-cyclic phosphate into 2′-phosphate (9).

We recently reported the crystal structures for CPDase (*A. thaliana*) in its oxidized (11), semi-reduced, and inhibitor-bound forms (12). The overall structure consists of two almost symmetrical lobes formed by the non-contiguous parts of the peptide chain, where each lobe consists of a three- or four-stranded antiparallel β-sheet that constitutes the inner core of the protein. The arrangement of the β-sheets resembles an open barrel flanked on the outside of each lobe by two anti-parallel α-helices. The active site is comprised of the tandem signature motif (residues His42, Thr44, His119, and Ser121) located in a water-filled cavity found within the core of the protein. A mutation study with the yeast CPDase revealed that the presence of the histidine residues of the signature motif is essential for the catalytic activity, but the threonine and serine residues are not, although their absence leads to partial inhibition of the catalytic activity (4).

The structure of the oxidized species of CPDase (*A. thaliana*) features two dithioether linkages formed by four of the six cysteine residues, as well as a flexible surface loop covering the active site. The flap-like shape of this loop is maintained by a disulfide bridge, formed by Cys104 and Cys110, tying together the upstream and downstream moieties of the loop. In the presence of DTT, we succeeded in crystallizing the semi-reduced species of CPDase, in which Cys104 and Cys110 were in their reduced states, while the other disulfide bridge remained intact. In the semi-reduced state, the N-terminal part of the surface loop folds into α-helical conformation, thereby elongating the preceding helix by two more turns (12).

The three phosphodiesterases investigated in this study do not share any significant amino acid similarity with each other; this is a common property of all members of this protein family. However, an alignment of the amino acid sequences is possible using the tandem signature motif as an anchor. It is tempting to speculate that despite these obvious differences, proteins of this family of phosphodiesterases adopt a similar fold, since their sizes are comparable and the spacing of the tandem signature motif is similar. In an attempt to recognize possible similarities between these enzymes and to gain further insight into molecular level mechanisms, we employed several biophysical methods for characterization of the three phosphodiesterases.

To compare structural features, we characterized urea-induced unfolding, native fluorescence, and oligomerization behavior of all three proteins. CD spectroscopy was used to investigate the general fold and possible effects of reducing agents or substrates. Furthermore, the enzymatic activity of the plant protein was elucidated using isothermal titration calorimetry with the wild type and four mutant proteins. The pos-

TABLE 1

Summary of Sedimentation Equilibrium Analyses

Sample	M in g/mol calculated	M in g/mol observed[a]
CPDase (*A. thaliana*)	21481	26100 (1800)
CPDase (*S. cerevisiae*)	28010	27700 (1900)
PDase Homolog/RNA ligase (*E. coli*)	21233	21000 (200)

Note. Standard deviations are given in parentheses.
[a] Experimentally determined M are averaged to the nearest hundred.

sible role of the redox-sensitive disulfide bridge located in the surface loop was also investigated.

MATERIALS AND METHODS

Cloning, expression, purification, and identification of recombinant proteins. Cloning and expression of the three proteins has been described previously. For CPDase (*A. thaliana*) wild type and mutants (His42Ala, Thr44Ala, His119Ala, Ser121Ala), constructs in pET11d were used for expression (2). The mutants were generated by PCR from the wild type plasmid with complementary primers carrying the desired mutation. The PCR products were digested with *Dpn*I and transformed into *E. coli* DH10B. For expression of CPDase (*S. cerevisiae*) a construct in pET28 was used (4). The cloning strategy for PDase Homolog/RNA ligase from *E. coli* was similar to the one used for the yeast CPDase, using *E. coli* DNA and appropriate PCR primers; this protein was also expressed from a construct with pET28. All three proteins carried C-terminal hexa-histidine tags and were purified by affinity chromatography using a Ni²⁺-nitrilotriacetic acid resin as described in (11).

The identity of the purified proteins was confirmed by N-terminal amino acid sequencing, which yielded the presence of Met1 for CPDase (*A. thaliana*), the absence of Met1 for CPDase (*S. cerevisiae*) and the absence of Met1/Val2 for the PDase Homolog/RNA ligase (*E. coli*). These results agree well with the molecular mass as determined by mass spectrometry (see Table 1) of diluted acidified samples using electrospray ionization on an HP1100 LCMS system (Agilent Technologies).

All proteins used were carefully checked by SDS–PAGE before further experiments; Coomassie staining indicated the presence of one band only.

Urea-induced unfolding. Folding stability of the three wild type proteins was investigated by urea-induced denaturation. The unfolding process was monitored by intrinsic fluorescence. Samples consisted of 2 μM protein in 100 mM NaCl, 30 mM TRIS (pH = 8.0) and had a total volume of 300 μl. Urea was present in 17 samples with concentrations ranging from 0 to 8 M. The samples were prepared 30 min prior to the measurements to allow for equilibration. Fluorescence emission spectra were recorded on a Perkin-Elmer LS 50B luminescence spectrometer using two excitation wavelengths, $\lambda_{exc} = 280$ nm and $\lambda_{exc} = 295$ nm, respectively. All fluorescence spectra were corrected against buffer-only samples and analyzed offline with the program AFDP (13). Three independent denaturing series were carried out for each protein. Each excitation set was analyzed by calculating an i-c(urea) relation, where i = $I(\lambda_{unfolded})/I(\lambda_{folded})$ (emission intensity analysis) and a λ-c(urea) relation (wavelength analysis).

Circular dichroism. Circular dichroic spectra were recorded with an AVIV 202 spectrometer. The final protein concentrations in the samples were 2 μM. For each sample, three CD spectra were collected and averaged and corrected offline with the program ACDP (13). Correction for each spectrum was against the respective buffer-only spectrum.

Analytical ultracentrifugation. A Beckman Optima Model XL-A analytical ultracentrifuge equipped with a four-place An-Ti rotor was used for sedimentation equilibrium experiments. Three 12 mm cells equipped with carbon-filled, double channel centerpieces and plane quartz windows were used. Protein solutions with absorbances at 280 nm ranging from 0.15 to 0.45 were loaded on the right (200 μl/channel) with the corresponding reference buffer on the left (220 μl/channel). The reference buffer was the dialysate buffer which contained 100 mM NaCl and 20 mM Tris (pH 8.0); $\rho = 1.003$ g/ml at 20.0°C, as determined with an Anton Paar Model DMA 58 densitometer. After equilibration at 3,000 rpm and 20.0°C at which reference wavelength and radial scans were performed, the rotor was accelerated to the selected experimental speed where the scans of protein concentration profiles were collected at 4 h intervals for 72 h. The proteins were run at two speeds: 17000 and 20000 rpm for CPDase (*A. thaliana*), 14000 and 17000 rpm for CPDase (*S. cerevisiae*), and 18000 and 21000 rpm for PDase Homolog/RNA ligase (*E. coli*), respectively. Radial scans were recorded at 280 nm in a step mode with 0.001 cm steps and 11 averages. Equilibrium was attained typically after 40–44 h, when two consecutive scans taken 4 h apart were indistinguishable. After the data collection was complete, the rotor was accelerated to 40000 rpm for 4–5 h and the protein sedimented to the bottom of the cell. The experimental centrifuge speed was restored and the baseline absorption values were immediately obtained from a single scan. Analysis of ultracentrifugation data was performed with the software package from Beckman, Inc., and A. P. Minton (NIDDK, NIH). Partial specific volumes of 0.710 ml/g for CPDase (*A. thaliana*); 0.719 ml/g for CPDase (*S. cerevisiae*); and 0.729 ml/g for PDase Homolog/RNA ligase (*E. coli*), respectively, were calculated from amino acid sequences and the values of Zamyatnin (14).

Isothermal titration calorimetry. Enzyme-substrate interaction enthalpies were determined using an isothermal titration calorimeter VP-ITC from MicroCal, LLC (Northampton, MA). Enzyme solutions with concentrations of either 0.01 mM or 0.1 mM were placed into the calorimetry cell (volume: 1.4199 ml) and the titration syringe contained a solution of 2′,3′-cAMP with either 0.1 mM or 1 mM concentration. The buffer used for enzyme and substrate solutions consisted of 100 mM NaCl, 5 mM TRIS (pH = 8.0), 0.1% NaN$_3$. For reducing conditions, 5 mM β-mercaptoethanol were added. The experiments were performed at 25°C by titration with 10 μl portions; titrations were repeated at least eight times for statistical purposes. For every regular titration, a reference experiment was carried out by titrating substrate into plain buffer. Offline analysis was performed using the program Origin 5.0 (MicroCal) with a special module for ITC data treatment. Low intensity signals were integrated directly from the raw data with Microsoft Excel 2000.

RESULTS

Folding Stability

Urea-induced unfolding as monitored by intrinsic fluorescence revealed a simple two-state unfolding reaction for all three proteins (see Fig. 1). One therefore can conclude that the proteins display a compact structure denaturing as one (un)folding unit. This behavior also allows for a stability analysis (Table 2) according to Pace (15), yielding the free stability energy for each protein, $\Delta G(H_2O)$.

Comparing the unfolding properties of the three phosphodiesterases we find the three proteins to be different from each other. While the CPDase from *Arabidopsis* (Fig. 1A) seems to be the most unstable protein in this series, the yeast CPDase (Fig. 1B) appears
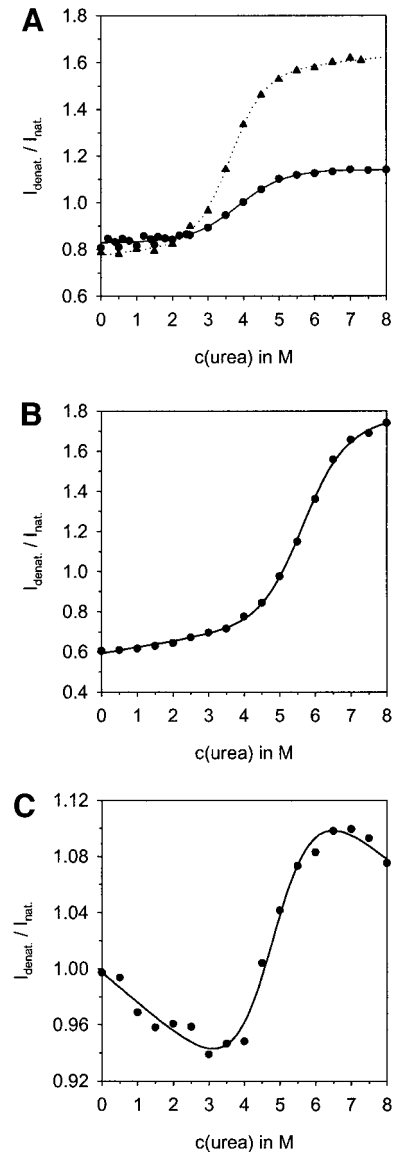

FIG. 1. Urea-induced denaturation of the three phosphodiesterases. (A) Unfolding of oxidised (circles) and semi-reduced (triangles) CPDase (*A. thaliana*). Semi-reducing conditions were achieved by the presence of 1 mM β-mercaptoethanol. (B, C) The unfolding of CPDase (*S. cerevisiae*) and the PDase Homolog/RNA ligase (*E. coli*), respectively. Fitted curves are superimposed on each scatter plot. The data shown in this graph were obtained from emission intensity analysis with excitation at $\lambda_{exc} = 280$ nm (see Materials and Methods) and are the average from three independent measurements.

to be the most stable one with a free stability energy about 50% higher than for the *Arabidopsis* enzyme. For both proteins the m values indicate comparable accessibility by the denaturant. In this series, the PDase Homolog/RNA ligase (*E. coli*) (Fig. 1C) takes the middle position with the free stability energy being 10% higher than for CPDase (*A. thaliana*). However, the unfolding curve shows two noteworthy differences: The slopes in the folded and unfolded region, respectively,

TABLE 2

Folding Stability

	Pace analysis[a]			λ analysis[b]
	$\Delta G(H_2O)$ kJ/mol	m kJ*l/mol^2	$c_{1/2}$(urea) M	$c_{1/2}$(urea) M
CPDase (*A. thaliana*), oxidised[c]	13.1	3.53	3.8	4.2
CPDase (*A. thaliana*), semi-reduced[c,e]	12.4	3.31	3.8	3.6
CPDase (*S. cerevisiae*)[c]	19.6	3.51	5.6	5.4
PDase Homolog/RNA ligase (*E. coli*)[d]	14.5	3.00	4.8	4.6

[a] For Pace analysis, intensity emission data were used as described in materials and methods.
[b] $c_{1/2}$ determined from the observed wavelength shift.
[c] Values represent the average from two sets of experiments, 280 nm and 295 nm excitation wavelength, respectively.
[d] Data obtained from 280 nm excitation only.
[e] Buffer addition: 1 mM β-mercaptoethanol.

show considerable slopes, and at the same time the m value is much lower than for the two CPDases. Comparing the results from unfolding experiments with CPDase (*A. thaliana*) in the oxidized and semi-reduced state shows only an insignificant difference of 5% in $\Delta G(H_2O)$ and no difference at all for $c_{1/2}$(urea).

Influences on the Protein Fold as Measured by CD Spectroscopy

Comparing the circular dichroism of the three phosphodiesterases shows that the spectra for the *Arabidopsis* (Figs. 2A and 2B) and the *E. coli* (Fig. 2E) protein are similar. While the PDase Homolog/RNA ligase possesses a slightly higher specific ellipticity than the plant protein, their overall spectra show the typical shape of mixed (α/β)-proteins, with intermixed secondary structure elements that often alternate along the polypeptide chain (16). The yeast protein (Figs. 2C and 2D), however, exhibits a different kind of CD spectrum, usually found for ($\alpha + \beta$)-proteins, which have two separate domains, one with mainly α- and one with mainly β-structure (16). The CD spectra of ($\alpha + \beta$) proteins usually have a larger intensity in the 210 nm band than in the 222 nm band; the reverse is true for (α/β) proteins and the minimum is always skewed towards the 222 nm band when there is a broad minimum (17).

Using the molar ellipticity at 222 nm and 208 nm, the *Arabidopsis* CPDase does not show significant differences in the presence or absence of Appr > p (Fig. 2B) in the pH range of 6–8. The same result is obtained with the yeast CPDase and 2′,3′-cAMP (Fig. 2D). Hence, CD spectroscopy does not indicate structural changes of the two CPDases upon addition of substrates.

This is different with the reducing agent DTT. While the *Arabidopsis* protein still exhibits the same CD spectrum (Fig. 2A), the specific ellipticity in case of the yeast protein (Fig. 2C) increases significantly while the shape of the spectrum still indicates ($\alpha + \beta$)-structure. This result for CPDase (*A. thaliana*) is remarkable,

since the crystal structure shows a conformational rearrangement of residues 100–115 leading to an extended α-helical element in the semireduced state (12). However, the additionally gained percentage of helical content is not significant enough to be detected by CD. pH variations from 3 to 9 and variations in ionic strength did not lead to significant changes in CD spectra of each of the three proteins (data not shown).

Native Fluorescence

Evaluation of the native fluorescence of proteins can give insights into the structural organization of the fluorophore groups. Comparing the fluorescence emission of excitation and emission spectra, CPDase from *A. thaliana* displays significantly lower intensities in the latter (43% at 280 nm excitation; see Fig. 3A), a phenomenon that is usually attributed to intrinsic protein fluorescence quenching. Correlating this finding with the three-dimensional structure, a possible explanation arises from the close spatial arrangement of Trp12 and Trp171 within the active site cleft of this CPDase (4 Å ring-to-ring distance). Additionally, four of the six tyrosine residues of this protein are distributed around the active site cavity with distances varying from 4.5 to 14 Å from the active site center. The yeast CPDase, by contrast, does not show any intrinsic fluorescence quenching since the excitation and emission spectra reveal the same intensities (Fig. 3B). Minor self-quenching is observed with the PDase Homolog/RNA ligase (Fig. 3C). Intrinsic protein fluorescence was monitored during titrations of 2′,3′-cAMP and Appr > p into samples containing the yeast or the plant CPDase; however, the observed effects were small and difficult to interpret, because of the presence of multiple fluorophores in the protein (data not shown).

Sedimentation Equilibrium Analysis

For determination of protein molecular weights and the states of aggregation, the sedimentation equilib-
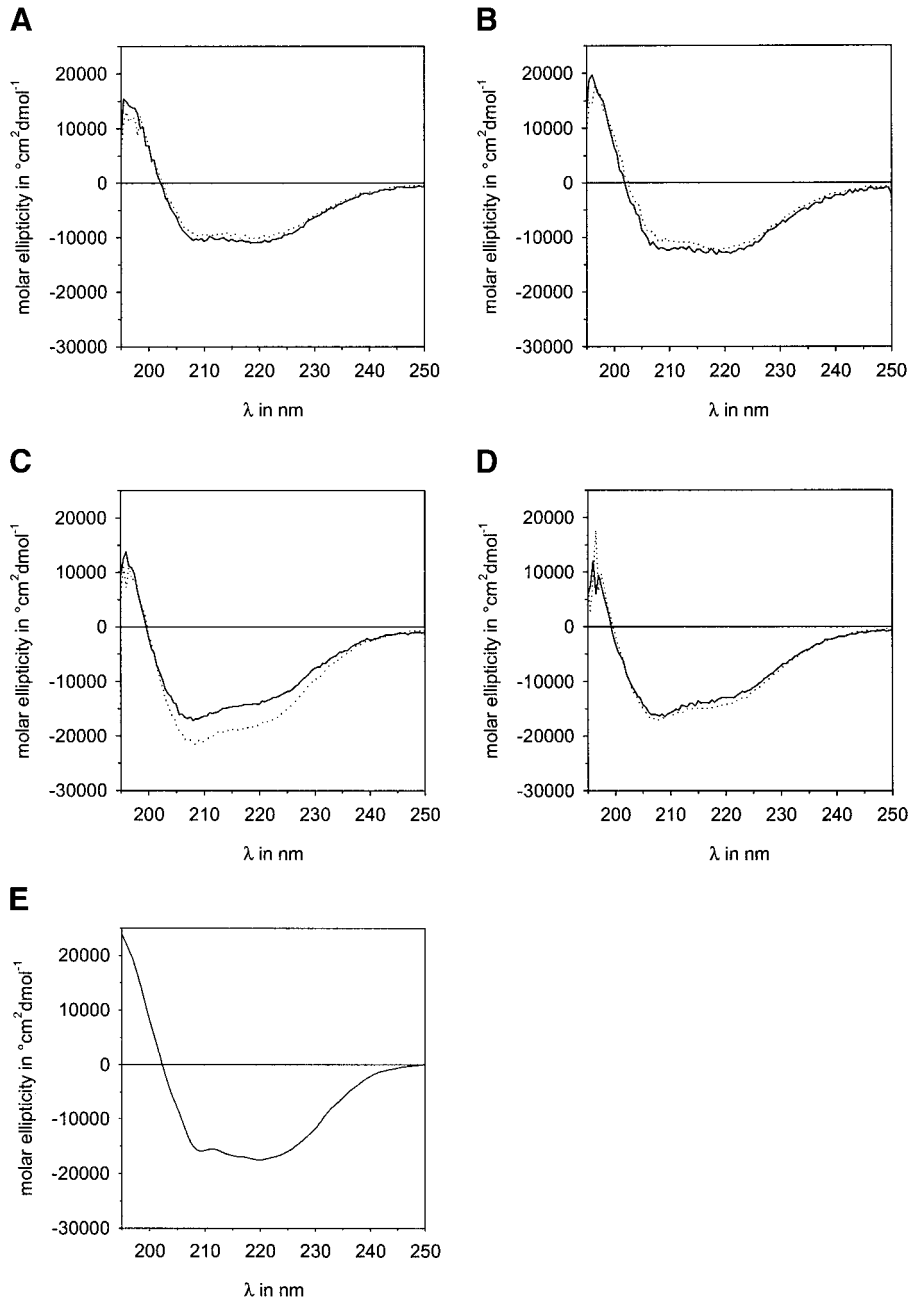
FIG. 2. Effects on the protein fold as determined by CD spectroscopy. CD spectra of 3 μM CPDase (*A. thaliana*) in the presence (dotted line) and absence (solid line) of 1 mM DTT (A) and 43 μM Appr > p (B). In the lower panel the CD spectra of 4 μM CPDase (*S. cerevisiae*) are shown in the presence (dotted line) and absence (solid line) of 1 mM DTT (C) and 0.14 mM 2′,3′-cAMP (D). The CD spectrum of the PDase Homolog/RNA ligase (*E. coli*) is shown in (E) for comparison. The buffer in every experiment contained 100 mM NaCl and 5 mM HEPES (pH = 7.0), except for (E) where 1% glycerol was present as well. All spectra were corrected against the respective buffer-only spectra and averaged from three consecutive scans.

rium analysis was employed (see Table 1). The data sets corresponding to the three protein concentrations obtained at a single centrifuge speed were analyzed initially using a single species ideal model. In case the global fits provided by this model were unacceptable (high and non-randomly distributed residuals), self-association models (monomer-dimer, etc.) were tested.

For CPDase (*A. thaliana*) the weight-average molecular weight was found to be 26100 g/mol, which is substantially higher than that for the ideal monomer (21481 g/mol). The distribution of the residuals was non-random and suggested typical association behavior. Hence, a self-association model assuming monomer-dimer equilibrium was tested and provided satis-
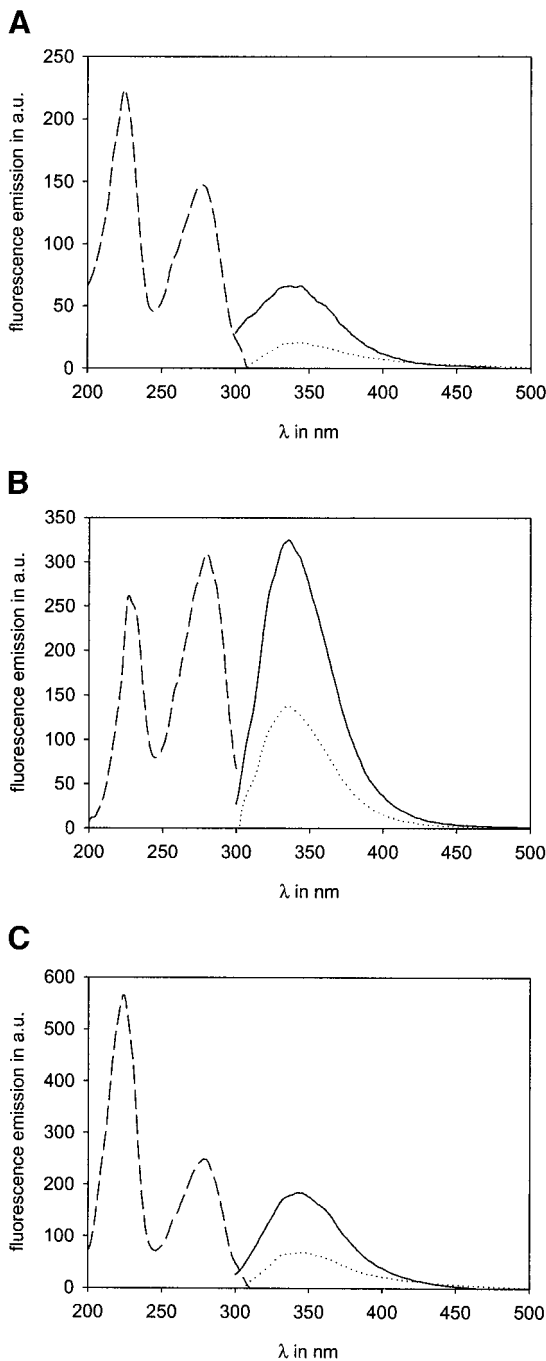
FIG. 3. Intrinsic protein fluorescence. Intrinsic fluorescence for (A) CPDase (*A. thaliana*), (B) CPDase (*S. cerevisiae*), and (C) PDase Homolog/RNA ligase (*E. coli*). Excitation spectra (λ_{em} = 350 nm) are plotted in dashed lines. Emission spectra for λ_{exc} = 280 nm are shown in solid lines and for λ_{exc} = 295 nm in dotted lines.

fractions of the dimer in the mixture were only 12%, 17%, and 21%, respectively.

The weight-average molecular weight for CPDase (*S. cerevisiae*) was found to be 27700 g/mol, which agrees well with the sequence molecular weight for the monomer (28010 g/mol). The sample behaved ideally during the ultracentrifuge run and the equilibrium was attained without any change in the molecular weight. The same observation was made with the PDase Homolog/RNA ligase (*E. coli*), indicating that both proteins exist as monomers in solution.

Enzyme-Substrate Interaction Enthalpy

2′,3′-cAMP was used as a model substrate for this study because of its easy availability. Titration of this substrate into a solution of wild type CPDase resulted in a significant exothermic effect (see Fig. 4). In contrast, three of the mutant proteins (Thr44Ala, His119Ala, Ser121Ala) displayed only marginal exothermic effects; with the mutant His42Ala a very small exothermic effect was observed.

Comparing the interaction enthalpies of oxidized and (semi-)reduced CPDase with 2′,3′-cAMP only a minor difference was found. The interaction enthalpy of the semi-reduced species with the substrate was about 8% less than the one found with the oxidized species.

DISCUSSION

Structural Characterization

An extensive intrinsic fluorescence quenching is observed with the plant CPDase. This can be readily explained on the basis of the crystal structure, since the two tryptophan residues are found to be in very close vicinity, while a ring-like distribution of tyrosine residues around the active site might also contribute to this effect. The yeast CPDase, by contrast, exhibits no fluorescence quenching at all. It is of particular interest that both tryptophan residues from the *Arabidopsis* protein are conserved in the yeast protein. Assuming that the fold for both proteins is the same, one should expect a similar effect between the two tryptophan residues in the yeast protein. However, CPDase (*S. cerevisiae*) possesses three additional tryptophan residues and one has to consider that these residues might overcompensate the quenching effect, although this seems very unlikely. Hence, one has to conclude that the conformation within the active site of the yeast protein differs from the one found in CPDase (*A. thaliana*). Alternatively, if the quenching observed in the case of the *Arabidopsis* protein is due to the quenching of tyrosine emission by the tryptophan residues, this phenomenon cannot be expected with the yeast CPDase since the ring-like distribution of tyrosine residues around the active site cleft is missing.
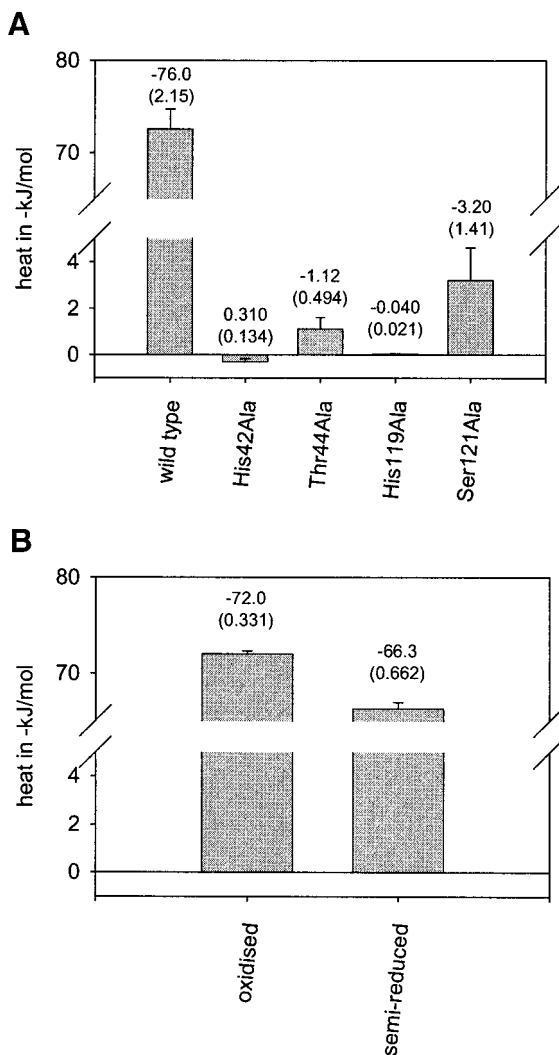
factory fits. The analysis yielded dimerization K_a value of only (7.7 ± 2.7) × 10^4 M^{-1} at 20°C, which indicated that the homodimer was in fact only moderately stable. For instance, for the protein concentrations used in the experiment (9.9 mM, 15.6 mM, and 22.8 mM), the

A

B

FIG. 4. Results from ITC experiments with CPDase (*A. thaliana*) wild type and mutants. The test substrate for this experiment series was 2′,3′-cAMP. Interaction enthalpies in kJ/mol are given on top of the bars; the values in parentheses represent the standard deviations.

The comparison of unfolding behavior for the three proteins within this study reveals distinct differences between them. There is a clear distinction between the values of the free stability energy (or the halfpoints of titration, $c_{1/2}$(urea)). A major difference between the plant and the yeast protein is the insertion of 30 amino acids in the $\beta 4$ region and thus at least one more structural element which contributes to the unfolding behavior. Secondly, cystine formation is a well-known contribution to protein stability. While the plant and yeast CPDases mentioned here possess six cysteine residues, the PDase Homolog/RNA ligase has only one cysteine residue and therefore cannot display intramolecular cystine formation. Since CPDase (*A. thaliana*) can exist in an oxidized and a semi-reduced state, and thus have either one or two disulfide bridges present,

one would expect it to be far more stable than the PDase Homolog/RNA ligase. However, both proteins possess approximately the same stability energies, although $c_{1/2}$(urea) for the *E. coli* protein is much higher.

The unfolding behavior of CPDase (*A. thaliana*) in the semi-reduced state (as assumed under conditions of 1 mM β-mercaptoethanol) displays a rather insignificant drop of about 5% in the free energy of stability as compared to the oxidized species. This result can be explained by the balance of different phenomena: The oxidized state of the protein shows a loop structure in the stretch 100–115, which should be easier to unfold than the α-helical structure found with the semi-reduced state. On the other hand, the loop is stabilized by the disulfide bridge Cys104–Cys110, which is not formed in the semi-reduced state. Both of these features seem to compensate each other, resulting in only insignificant differences of the free stability energy.

As mentioned above, the yeast CPDase also carries six cysteine residues like the *Arabidopsis* protein, although the positions within the sequences are not conserved. Since structural information about CPDase (*S. cerevisiae*) is not available, one can only speculate about the redox state of these residues. While mass spectrometry did not detect the absence of protons which would indicate the presence of one or more disulfide bridges, we think that the high stability energy within the series of the three proteins investigated in this study gives reason to assume at least one cystine is present under non-reducing conditions, particularly since the CD spectrum of CPDase (*S. cerevisiae*) exhibits a sensitivity towards reducing agents. Furthermore, the additional structural element in the yeast protein (due to an insertion of about 30 residues) might also contribute to the higher stability as compared to the *Arabidopsis* CPDase.

The conclusions to be drawn from the native CD spectrum of CPDase (*A. thaliana*) agree very well with the fold found in the crystal structure. The redox-dependent conformational change within the surface loop provokes the absence or presence of two additional helical turns which is too low to be detected in the CD spectrum. The yeast CPDase, however, presents itself as a different fold in the CD spectrum, the shape of which is usually interpreted as an ($\alpha + \beta$) fold. Additionally, reducing conditions lead to a significant increase of specific ellipticity which indicates redox-induced conformational changes.

Functional Characterization

ITC experiments that have been performed in this study address two questions: the comparison of the wild type CPDase with four mutants is to prove the validity of our previous hypothesis that residues His42, Thr44, His119, and Ser121 are critical for the catalytic reaction. This hypothesis was supported by the crystal

structure (11, 12) and a mutagenesis study with CPDase (*S. cerevisiae*) (4). Based on the current results, it is absolutely clear that these four residues are essential for the catalytic reaction since variation in either one of the four positions leads to almost complete reduction of interaction enthalpy. However, the plant and the yeast enzyme differ in one detail: While mutations of the assisting residues Thr41 and Ser152 in case of the yeast enzyme inhibit the catalytic activity only partially, depending on the nature of the substrate used (4), these residues in the plant enzyme play a much more important role. Both mutants, Thr44Ala and Ser121Ala, exhibit interaction enthalpies around zero. Therefore, in case of the plant CPDase, all four residues of the tandem signature motif are essential for enzymatic activity. Since the assignment of an assisting role to the threonine/serine residues in the catalytic reaction seems still reasonable, a different structural environment in the active site of both proteins could account for this functional difference. While the plant enzyme needs these assisting residues in order to orient the substrate correctly in the active site, the yeast protein might possess additional structural features which fulfill this role. This scenario would ascribe less importance to the assisting residues in the yeast CPDase and thus explain the current findings.

Secondly, a question of interest is certainly whether the actual redox state of CPDase (*A. thaliana*) impacts the catalytic reaction. For this purpose, the wild type enzyme was subjected to the same ITC protocol in the absence and in the presence of a reducing agent. In this experiment, the semi-reduced species produced about 8% less interaction enthalpy with the test substrate (2′,3′-cAMP) than the oxidized species. While the catalytic reaction itself was not expected to be influenced by the redox state (11), the different conformations of the surface loop (residues 100–115) in either the oxidized or semi-reduced state gave rise to the question whether there might be a peripheral effect on the enzymatic function. This seemed very probable because any attempt to co-crystallize a substrate or an inhibitor with CPDase (*A. thaliana*) was unsuccessful with the oxidized form. However, the discovery of the semi-reduced form allowed us to co-crystallize cyclic uridine-vanadate with the protein. In light of the current finding, one has to conclude that the redox state of CPDase is not important for its enzymatic activity.

CONCLUSION

This study provides, for the first time, a comparison of biophysical properties for three cyclic nucleotide phosphodiesterases, the CPDases from *A. thaliana, S. cerevisiae,* and the PDase Homolog/RNA ligase from *E. coli.* The results for the plant CPDase are in excellent agreement with the recently reported crystal structures and with the proposed catalytic mechanism (11,

12). ITC experiments proved that all four residues of the tandem signature motif are essential for the catalytic activity of the plant CPDase; this is somewhat different in the yeast CPDase where only the histidine residues have been reported to be essential (4). The redox-dependent conformation of the surface loop does not seem to impact the catalytic activity of the plant CPDase. The conformational change as seen in the crystal structures (12) could not be observed by CD spectroscopy, probably because of the rather small changes in helical content. Judging from the experiments within this study the PDase Homolog/RNA ligase seems to be more similar to the plant than to the yeast CPDase. Based on intrinsic protein fluorescence, CD spectra and the previously reported (4) roles of the residues of the tandem signature motif in catalytic activity, the yeast protein clearly appears to be distinct from the plant protein. A different overall structure (or at least a different arrangement of the periphery of the protein) than in the case of the plant CPDase does not seem unlikely. Crystallization attempts are under way for CPDase (*S. cerevisiae*) in order to obtain detailed structural information.

REFERENCES

1. Culver, G., McCraith, S., Zillmann, M., Kierzek, R., Michaud, N., LaReau, R., Turner, D., and Phizicky, E. (1993) An NAD derivative produced during transfer RNA splicing: ADP-ribose-1″,2″-cyclic-phosphate. *Science* **261,** 206–208.

2. Genschik, P., Hall, J., and Filipowicz, W. (1997) Cloning and characterization of the *Arbidopsis* cyclic phosphodiesterase which hydrolyses ADP-ribose 1″,2″-cyclic phosphate and nucleotide 2′,3′-cyclic phosphates. *J. Biol. Chem.* **272,** 13211–13219.

3. Martzen, M. R., McCraith, S. M., Spinelli, S. L., Torres, F. M., Fields, S., Grayhack, E. J., and Phizicki, E. M. (1999) A biochemical genomics approach for identifying genes by the activity of their products. *Science* **286,** 1153–1155.

4. Nasr, F., and Filipowicz, W. (2000) Characterisation of the *Saccharomyces cerevisiae* cyclic nucleotide phosphodiesterase involved in the metabolism of ADP-ribose 1″,2″-cyclic phosphate. *Nucl. Acids Res.* **28,** 1676–1683.

5. Zillmann, M., Gorovsky, M. A., and Phizicky, E. M. (1991) Conserved mechanism of tRNA splicing in eukaryotes. *Mol. Cell. Biol.* **11,** 5410–5416.

6. Zillmann, M., Gorovsky, M., and Phizicky, E. (1992) HeLa cells contain a 2′-phosphate-specific phosphotransferase similar to an yeast enzyme implicated in tRNA splicing. *J. Biol. Chem.* **267,** 10289–10294.

7. Culver, G., Consaul, S., Tycowski, K., Filipowicz, W., and Phizicky, E. (1994) tRNA splicing in yeast and wheat germ. A cyclic phosphodiesterase implicated in the metabolism of ADP ribose. *J. Biol. Chem.* **269,** 24928–24934.

8. Tyc, K., Kellenberger, C., and Filipowicz, W. (1987) Purification

and characterisation of wheat germ 2′,3′-cyclic-nucleotide-3′-phosphodiesterase. *J. Biol. Chem.* **262,** 12994–13000.

9. Arn, E. A., and Abelson, J. N. (1998) RNA ligases: Function, mechanism and sequence conservation. *In* RNA Structure and Function (Simons, R., and Grunberg-Manago, M., Eds.), pp. 695–726, Cold Spring Harbor Laboratory Press, Cold Spring Harbor, NY.

10. Arn, E. A., and Abelson, J. N. (1996) The 2′–5′ RNA ligase of Escherichia coli. Purification, cloning, and genomic disruption. *J. Biol. Chem.* **271,** 31145–31153.

11. Hofmann, A., Zdanov, A., Genschik, P., Ruvinov, S., Filipowicz, W., and Wlodawer, A. (2000) Structure and mechanism of the cyclic phosphodiesterase of Appr > p, a product of the tRNA splicing reaction. *EMBO J.* **19,** 6207–6217.

12. Hofmann, A., Grella, M., Botos, I., Filipowicz, W., and Wlodawer, A. (2002) Crystal structures of the semi-reduced and inhibitor-bound forms of cyclic nucleotide phosphodiesterase from *Arabidopsis thaliana. J. Biol. Chem.* **277,** 1419–1425.

13. Hofmann, A., and Wlodawer, A. (2002) PCSB—Program collection for structural biology and biophysical chemistry. *Bioinformatics,* in press.

14. Zamyatnin, A. (1984) Amino acid, peptide, and protein volume in solution. *Annu. Rev. Biophys. Bioeng.* **13,** 145–165.

15. Pace, C. N. (1995) Evaluating contribution of hydrogen bonding and hydrophobic bonding to protein folding. *Methods Enzymol.* **259,** 538–554.

16. Venyaminov, S. Y., and Yang, J. T. (1996) Determination of protein secondary structure. *In* Circular Dichroism and the Conformational Analysis of Biomolecules (Fasman, G. D., Ed.), pp. 69–108, Plenum Press, New York.

17. Manavalan, P., and Johnson, W. C. (1983) Sensitivity of circular dichroism to protein tertiary structure class. *Nature* **305,** 831–832.